European Journal of Immunology

WILEY-VCH

European Journal of Immunology
Basic • Clinical • Translational

RESEARCH ARTICLE OPEN ACCESS

Allergy and Inflammation

Prophylactic Inhaled Pattern Recognition Receptor Agonists Reprogram Lung Epithelial Response and Prevent Type 2 Allergic Inflammation

Mbaya Ntita[1] | Celine Shuet Lin Kong[1] | Dalia Hassan[2] | Richa Nayak[3,4] | Jezreel Pantaleón García[1] | Yongxing Wang[1] | Jichao Chen[5] | Scott E. Evans[1]

[1]Department of Pulmonary Medicine, The University of Texas MD Anderson Cancer Center, Houston, Texas, USA | [2]Cold Spring Harbor Laboratory, New York, New York, USA | [3]Department of Cancer Biology, The University of Texas MD Anderson Cancer Center, Houston, Texas, USA | [4]Graduate School of Biomedical Sciences, UT MD Anderson Cancer Center UT Health Houston, Houston, Texas, USA | [5]Division of Pulmonary Biology, Department of Pediatrics, Cincinnati Children's Hospital Medical Center, Cincinnati, Ohio, USA

Correspondence: Scott E. Evans (seevans@mdanderson.org)

Received: 1 July 2025 | **Revised:** 27 February 2026 | **Accepted:** 2 March 2026

Keywords: lung epithelial cell | PRR agonists | reprogramming | Type 2 allergy

ABSTRACT

Prophylactic inhalation of the synergistic agents ODN M362 and Pam2CSK4 ("Pam2ODN") protects mice against allergic lung disease, including allergic inflammation caused by house dust mite (HDM). By preventing sensitization, Pam2ODN reduces HDM-induced eosinophilic and lymphocytic inflammation. How Pam2ODN affects interactions among lung epithelial cells, dendritic cells, and T cells to prevent eosinophilic lung inflammation remains unclear. In the present study, we show that a single inhaled dose of Pam2ODN before HDM sensitization reduces airway Th2 polarization without affecting Th1 or Treg responses. Furthermore, Pam2ODN pretreatment inhibits the recruitment of lung monocyte-derived dendritic cells (moDCs) and conventional Type 2 dendritic cells (DC2s), while preventing the HDM-induced decrease in conventional Type 1 dendritic cells (DC1s). Bulk RNA-seq of the whole lung reveals that Pam2ODN pretreatment restricts the expression of proinflammatory transcripts induced by HDM sensitization. This tolerogenic effect is also reflected at the single-cell level in lung epithelial cells, where proinflammatory transcripts, pathways, and chromatin accessibility are inhibited. These results indicate that Pam2ODN reprograms lung epithelial cells to attenuate allergen-induced Th2-promoting cytokines and DCs while maintaining the population of protective DC1s. These findings suggest a strategy to mitigate chronic allergic lung diseases.

1 | Introduction

Living in an urban environment has been linked to an increase in the prevalence of allergic sensitization and the development of allergic diseases [1]. Congruently, children who live in areas with low concentrations of microbial contaminants, such as lipopolysaccharide (LPS), are more likely to develop allergic T-helper Type 2 (Th2) cell responses [2]. Mechanistic studies have shown a protective effect against allergic Th2 cell responses by chronic exposure to microbial contaminants that is mediated by downregulation of inflammatory pathways in airway epithelial cells [3]. Th2 cell-induced allergic inflammation results from epithelial cell-associated molecules released upon the activation of epithelial pattern recognition receptors (PRRs) and their downstream molecules [4, 5]. Upon exposure to allergens, lung epithelial cells release inflammatory cytokines and alarmins that recruit and activate lung innate immune cells, including dendritic cells (DCs), monocytes, and macrophages. Via antigen

presentation, these cells activate and polarize naïve CD4$^+$ T cells towards a Th2 cell phenotype [6–8]. Allergen-specific Th2 cells and their associated cytokines IL-4, IL-5, and IL-13 that drive eosinophil infiltration are increased in the airways of asthmatic patients and mice with allergic eosinophilic inflammation, and their levels correlate with symptom severity [9–12].

We have previously reported in mice that survive acute Sendai virus pneumonia challenge that therapeutic inhalation of synergistic agents Pam2CSK4, a TLR2/6 ligand, and ODN M362, a TLR9 ligand that also binds RIG-I and VDAC1, protects against the late asthma-like chronic disease [13–15]. Further, we showed that the protection was independent of the impact of Pam2ODN on virus burden [13]. This prompted us to test several other mouse models of asthma, revealing that pretreatment with Pam2ODN also prevents airway eosinophilia, lymphocytic inflammation, mucus metaplasia, and airway hyperresponsiveness in non-infectious allergic models, suggesting that the treatment has a protective effect through blocking airway allergic sensitization [16]. While offering limited molecular insight, this earlier investigation demonstrated the protective effects of Pam2ODN against phenotypic allergen-induced airway remodeling and the preservation of lung function. However, the nature of the changes this treatment imprints on the lung epithelial cells that are primarily responsible for preventing allergic sensitization [17, 18] and how those changes subsequently affect the early immune responses of DCs and T cell polarization have not been established.

Using the clinically-relevant house dust mite (HDM) extract mouse model of allergic lung inflammation [19, 20], we show here that Pam2ODN-treated lung epithelial cells display epigenetic and transcriptomic reprogramming that is associated with an immunomodulatory response against subsequent HDM sensitization, resulting in reduced recruitment of Type 2 conventional and monocyte-derived DCs (moDCs), with fewer Th2 cells and eosinophils in the airways after HDM challenge. Importantly, Pam2ODN-Induced epithelial epigenetic imprinting has a long-lasting tolerogenic effect, as mice treated 30 days before HDM sensitization still exhibit reduced levels of both airway Th2 cells and eosinophils following HDM challenge. Altogether, these results demonstrate epigenetic reprogramming as a key mechanism of PRR agonist-induced tolerance against HDM sensitization and subsequent development of Th2 cell-induced airway eosinophilic allergic inflammation.

2 | Results

2.1 | Pam2ODN Pretreatment Blocks Airway Th2 Polarization and Eosinophilia

HDM extract-induced eosinophilic inflammation is associated with Th2 polarization [12, 20]. Since Pam2ODN, given before HDM sensitization, prevents allergic airway inflammation [16], we investigated whether Pam2ODN also prevents HDM-induced eosinophilic inflammation by regulating Th2 cells. We used an HDM model that causes T-helper-cell-mediated airway inflammation evocative of human asthma [19, 21]. BALB/c mice were sensitized by intratracheal instillation of 100 μg of HDM extract, followed by six daily nasal challenges of 10 μg HDM extract from Days 7 to 12. We evaluated the allergic inflammation in BAL fluid by flow cytometry on Day 14 in mice that received inhalation of PBS or Pam2ODN 7 days before HDM sensitization, and mice that received Pam2ODN 3 days after HDM sensitization (Figure 1A). Mice treated 21 days earlier with PBS or Pam2ODN alone (no HDM) served as controls. Consistent with our previous report [16], we confirmed that PBS-pretreated/HDM-sensitized/HDM challenged mice (PBS/HDM/HDM) and those treated with Pam2ODN 3 days after HDM sensitization (+3d Pam2ODN/HDM/HDM) exhibited an increased number of total airway leukocytes (Figure 1B) and an increased frequency and absolute number of eosinophils. This pattern was significantly attenuated in mice treated with Pam2ODN 7 days before sensitization and subsequent challenge (-7d Pam2ODN/HDM/HDM) (Figure 1C–E). Pam2ODN-treated control mice (no HDM) had fewer neutrophils than PBS-treated controls (Figure 1F,G). However, Pam2ODN didn't change neutrophil frequency in HDM-challenged mice (Figure 1G). We next assessed the effect of Pam2ODN treatment on the CD4$^+$ T cell polarization. The frequency and absolute number of Th2 cells were higher in PBS/HDM/HDM and +3d Pam2ODN/HDM/HDM than in -7d Pam2ODN/HDM/HDM mice (Figure 1I–K), indicating that Pam2ODN pretreatment prevented Th2 polarization. We observe only a modest effect of Pam2ODN pretreatment on airway ILC2s (Figure S2B). Th17 CD4$^+$ T cells that express RORγt and produce IL-17A, IL-17F, and IL-22 [22, 23] can synergize with Th2 CD4$^+$ T cells to induce either a severe phenotype of eosinophilic inflammation or to drive a non-Type 2 neutrophilic asthma [24, 25]. Moreover, at different stages of maturation, CD11b$^+$ conventional DCs that drive Th2 cell differentiation can also drive the differentiation of CD4$^+$ T cells towards a Th17 cell phenotype [26]. Pam2ODN administration before or after sensitization had no significant effect on the frequency or absolute number of Th17 cells (Figure 1L–N). Th1 CD4$^+$ T cells that express T-bet transcription factor and produce IFNγ [27] and Treg cells that express Foxp3 transcription factor and produce IL-10 and TGF-β [28, 29] can be involved in the regulation of the immune response to allergic inflammation by preventing the polarization of native CD4$^+$ T cells towards the Th2 or Th17 phenotype and lung allergic inflammation [30–33]. Unlike its effect on Th2 cell polarization, Pam2ODN treatment did not affect Th1 or Treg cell differentiation (Figure 1O,P,R,S). In -7d Pam2ODN/HDM/HDM mice, airway inflammatory cytokines in BALF were decreased, including the regulatory cytokine IL-10 (Figure S3), likely reflecting overall attenuation of the immunological response. The lack of significant effects on Th17, Th1, or Treg populations demonstrates that Pam2ODN pretreatment inhibits HDM-induced Type 2 allergic eosinophilic inflammation by moderating Th2 polarization.

2.2 | Long-Lasting Effect of Pam2ODN Against Allergen-Induced Airway Th2 Cell Polarization

We next investigated the long-term effect of Pam2ODN pretreatment on HDM-induced airway Th2 polarization and eosinophilic inflammation. We sensitized mice with 100 μg of HDM extract, and six daily nasal challenges of 10 μg of HDM extract were administered from Days 7 to 12, as above (Figure 1). On Day 14, we used flow cytometry to assess the allergic inflammation in BAL fluid in mice that inhaled PBS (PBS/HDM/HDM) or Pam2ODN (-30d Pam2ODN/HDM/HDM) 30 days before HDM sensitization, and mice that received Pam2ODN 3 days after HDM

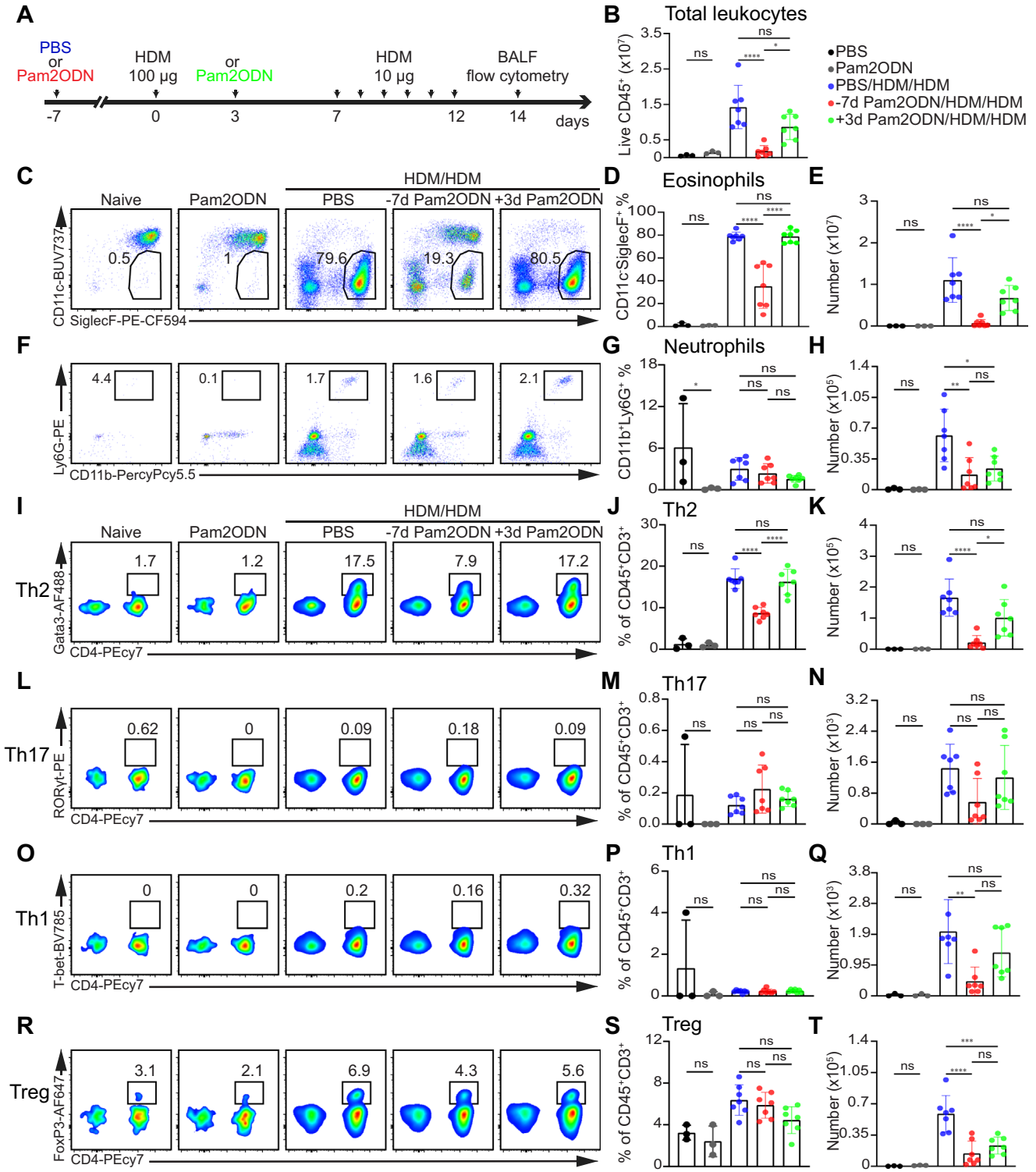

FIGURE 1 | Pam2ODN pretreatment attenuates airway Th2 polarization and eosinophilic inflammation. (A) Experimental design. A single aerosolized treatment of PBS or Pam2ODN was given seven days before the naïve mice's initial HDM sensitization, or a single dose of Pam2ODN was given 3 days after the mice's initial HDM sensitization. Flow cytometry was used to examine single-cell suspensions obtained from the bronchoalveolar lavage fluid (BALF) after challenges. (B) Summary graph of total airway leukocytes. (C) Flow cytometry plots and summary graph of airway eosinophil (D) percentage and (E) number. (F) Flow cytometry plots and summary graph of airway neutrophil (G) percentage and (H) number. (I) Flow cytometry plots and summary graph of airway Th2 (J) percentage and (K) number. (L) Flow cytometry plots and summary graph of airway Th17 (M) percentage and (N) number. (O) Flow cytometry plots and summary graph of airway Th1 (P) percentage and (Q) number. (R) Flow cytometry plots and summary graph of airway Treg (S) percentage and (T) number. Experiments were performed at least two times. $N = 3$–7 mice/group. Numbers within the representative flow cytometry plots indicate the percentage of each cell population. Bars show mean ±SD. $*p < 0.05$; $**p < 0.01$; $***p < 0.001$; $****p < 0.0001$; ns = not significant. Statistical analysis performed by GraphPad Prism using one-way ANOVA with Bartlett's test correction for multiple comparisons.

sensitization (+3d Pam2ODN/HDM/HDM) (Figure S4A). As in Figure 1, the number of total airway leukocytes was higher in PBS/HDM/HDM mice and +3d Pam2ODN/HDM/HDM mice (Figure S4B). The frequency and absolute number of eosinophils were lower in -30d Pam2ODN/HDM/HDM mice compared to PBS/HDM/HDM (Figure S4C–E). PBS/HDM/HDM and +3d Pam2ODN/HDM/HDM mice also had higher frequencies and absolute numbers of Th2 cells than -30d Pam2ODN/HDM/HDM mice (Figure S4F–H), without significant effects on Th17, Th1, or Treg cells (Figure S4F–T), indicating that Pam2ODN pretreatment has a durable tolerogenic effect against HDM-induced Th2 polarization that persists for at least a month.

2.3 | Pam2ODN Modulates Lung DC Responses to HDM Sensitization

DCs and monocytes critically interact with airway epithelial cells in the establishment of allergic lung inflammatory diseases [8]. In asthma, Th2 cell responses to inhaled allergens are initiated and maintained by DCs [8, 34]. Conventional $CD11c^+MHCII^+$ DCs (cDCs) are essential to HDM extract uptake and antigen presentation. Two ontogenically distinct subsets of conventional DCs play different roles in allergic inflammation [34, 35]. Type 2 conventional DCs (DC2s), whose development depends on the transcription factor IRF4, efficiently take up and present HDM allergens, promoting allergic inflammation by activating naïve T cells and promoting full Th2 differentiation in mediastinal lymph nodes [34, 36]. Type 1 conventional DCs (DC1s), whose development depends on IRF8 and Batf3 [37, 38], play a regulatory role by promoting tolerogenic immune responses against allergic lung sensitization through IL-12 expression and by inducing Treg differentiation [39, 40]. moDCs expressing $CD11b^+Ly6C^+CD11c^+MHCII^+$ also promote Th2 polarization in the high-dose HDM model and significantly contribute to allergic sensitization [34]. We evaluated the impact of Pam2ODN pretreatment on early lung DC immune responses to HDM sensitization. PBS- (PBS/HDM) or 7-day Pam2ODN (-7d Pam2ODN/HDM)-pretreated mice were given 100 μg of HDM intratracheally, and DC activation was assessed 24 h later. The total population of conventional DCs was higher in PBS/HDM compared to -7d Pam2ODN/HDM and naïve controls (Figure 2A–C), suggesting that Pam2ODN pretreatment has an immunomodulatory effect on the activation and recruitment of cDCs. Compared to naïve control mice, PBS/HDM mice had fewer DC1s, as previously reported [41], while Pam2ODN pretreatment prevented the HDM-induced reduction in DC1s (Figure 2D–F). In contrast to naïve control mice, both PBS/HDM and -7d Pam2ODN/HDM mice had increased DC2s (Figure 2D,G,H). However, -7d Pam2ODN/HDM mice had significantly lower levels of DC2s than PBS/HDM mice (Figure 2D,G,H). HDM exposure also increased the population of moDCs. Compared to naïve control mice, both PBS/HDM and -7d Pam2ODN/HDM mice had an increased moDCs (Figure 2I–K). -7d Pam2ODN/HDM mice had also significantly fewer moDCs than PBS/HDM mice (Figure 2I–K). When we analyzed migratory DCs (mig-DCs) in mediastinal lymph nodes 4 days after HDM sensitization, -7d Pam2ODN/HDM mice still had significantly fewer DC2s and higher DC1s than PBS/HDM mice (Figure S5E–G). Taken together, these findings indicate that Pam2ODN pretreatment inhibits recruitment and activation of DC2s and moDCs that cause allergic sensitization while maintaining the population of protective DC1s, thereby preventing airway Th2 cell polarization and eosinophilic inflammation.

2.4 | Pam2ODN Suppresses HDM-Induced Allergic Inflammatory Transcripts

Th2-polarizing activated DCs respond to inflammatory mediators released in the lung environment upon sensitization, such as CCL2, CCL20, IL-33, IL-25, TSLP, IL-1β, IL-1α, and GM-CSF [42, 43]. We next used bulk RNA-seq analysis of whole-lung homogenates to investigate the effect of Pam2ODN on HDM-sensitization-induced inflammatory gene expression (Figure 3A). Principal component analysis of the transcriptional responses separated control PBS/PBS from HDM-inflamed samples, and PBS/HDM clustered far from control PBS/PBS compared to samples from mice that received Pam2ODN before HDM sensitization (-7d Pam2ODN/HDM) (Figure 3B), suggesting a regulatory effect of Pam2ODN on HDM-induced lung transcriptomic changes. PBS pretreatment followed by HDM sensitization resulted in 883 differentially expressed genes (DEGs) compared to PBS/PBS (Figure 3C). However, Pam2ODN pretreatment followed by HDM sensitization resulted in fewer induced genes, including 137 uniquely regulated genes (Figure 3C), demonstrating a broad immunomodulatory effect of Pam2ODN on the transcriptional response to HDM. In fact, Figure 3D shows that Pam2ODN-pretreatment downregulates most genes that were upregulated in PBS/HDM mice and upregulates most that were downregulated in PBS/HDM mice (Figure 3D). Comparison of DEGs (FDR < 0.05, absolute fold change ≥ 2) shows that -7d Pam2ODN/HDM mice had fewer upregulated genes (30 genes) and more downregulated genes (58 genes) (Figure 3E). Relative to the PBS/PBS control condition, most of the HDM sensitization-induced cytokines, chemokines, and chemokine receptor genes, including those involved in the recruitment and activation of DCs, were attenuated in -7d Pam2ODN/HDM mice (Figure 3F), confirming the immunomodulatory and tolerogenic effects of Pam2ODN against lung HDM sensitization. In addition, Pam2ODN pretreatment attenuated the expression of several inflammatory innate immune genes and transcription factors, including Tlr2, Arg2, Irf7, Cd14, Myd88, Nlrp3, and Socs3, which play critical roles in lung allergic inflammation (Figure 3G). An analysis of the top 15 gene ontology (GO) pathway enrichments classifies the inflammatory response into the pathways most restricted by Pam2ODN. Notably, this analysis also shows that Pam2ODN pretreatment restricts the positive regulation of Th2 cell cytokine production and the positive regulation of Th2 cell differentiation pathways (Figure 3H). Altogether, these data suggest that Pam2ODN pretreatment prevents HDM sensitization-induced lung inflammatory immune response that drives the activation of DCs required for the lung allergic sensitization.

2.5 | Lung Epithelial Cells Exhibit Tolerogenic Reprogramming

While DCs serve as a link between the lung's innate and adaptive immune responses during allergic initiation, airway allergens initially interact with the respiratory epithelium, which responds

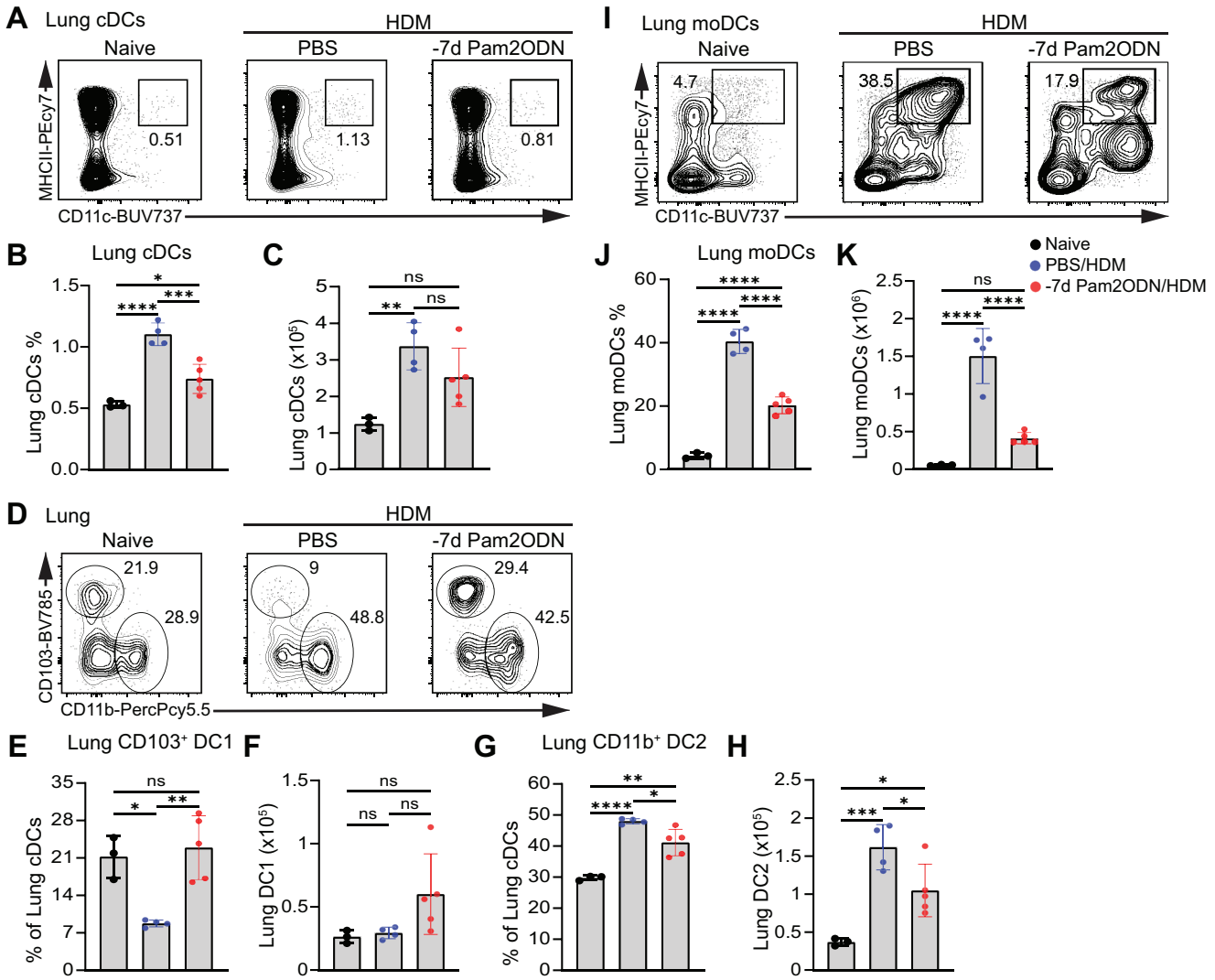

FIGURE 2 | Pam2ODN pretreatment modulates lung DC recruitment at the time of HDM sensitization. Seven days before intratracheal sensitization with HDM, naïve mice received a single aerosol treatment of PBS or Pam2ODN. Twenty four hours after the HDM was administered, whole lungs were removed, and single-cell suspensions were made for flow cytometry analysis. (A) Flow cytometry plots and summary graph of lung conventional dendritic cells (cDCs) (B) percentage and (C) number. (D) Flow cytometry plots of lung cDCs subsets DC1 and DC2. (E) Summary graph of lung conventional DC1 percentage and (F) number. (G) Summary graph of lung conventional DC2 percentage and (H) number. (I) Flow cytometry plots and summary graph of lung moDCs (J) percentage and (K) number. Experiments were performed at least two times. $N = 3–5$ mice/group. Numbers within the representative flow cytometry plots indicate the percentage of each cell population. Bars show mean ± SD. $*p < 0.05$; $**p < 0.01$; $***p < 0.001$; $****p < 0.0001$; ns = not significant. Statistical analysis was performed by GraphPad Prism using one-way ANOVA with Bartlett's test correction for multiple comparisons.

by releasing inflammatory mediators that recruit and activate Th2 cell-polarizing DCs [18]. Given this important epithelial role, we performed single-cell transcriptional analysis to examine how Pam2ODN affects lung epithelial cell responses to HDM. Two pairs (one male and one female each) of mice were given 100 μg of HDM intratracheally 12 h before lung harvest for analysis, and one pair received an inhalation of Pam2ODN 7 days before HDM exposure. FACS-sorted lung epithelial cells were submitted for scRNA-seq analysis (Figure S6A). Epithelial cell populations were defined by expression of canonical markers for Type 1 alveolar epithelial cells AT1 (*Rtkn2*), Type 2 alveolar epithelial cells AT2 (*Sftpc*), AT2/AT1 transitioning (*Cav1*), and airway epithelial cells (*Sox2*) (Figure 4A). While AT2 cells were the most abundant epithelial cell type, as reported [44] in both conditions, we observed a remarkable shift of the AT2 cell type and higher frequency of AT2/AT1 transitioning cells in -7d Pam2ODN/HDM mice than in PBS/HDM mice (Figure 4B,C; Figure S6B,C), suggesting transcriptional reprogramming response to HDM and an early activation of the epithelial repair process by Pam2ODN pretreatment, respectively [45, 46]. PBS/HDM mice had slightly higher AT1 cell fractions, and airway cell fractions were similar in both conditions (Figure 4B,C). The identity of these cell types was confirmed by the abundance of additional canonical markers (Figure 4D). Since AT2 cells play a major role in the initiation of lung allergic inflammation and can be responsive to therapies such as glucocorticoids [47, 48], we next compared differential gene expression in AT2 cells from PBS/HDM and -7d Pam2ODN/HDM mice. Pam2ODN pretreatment inhibits the expression of many inflammatory genes induced by HDM (Figure 4E). Among the 176

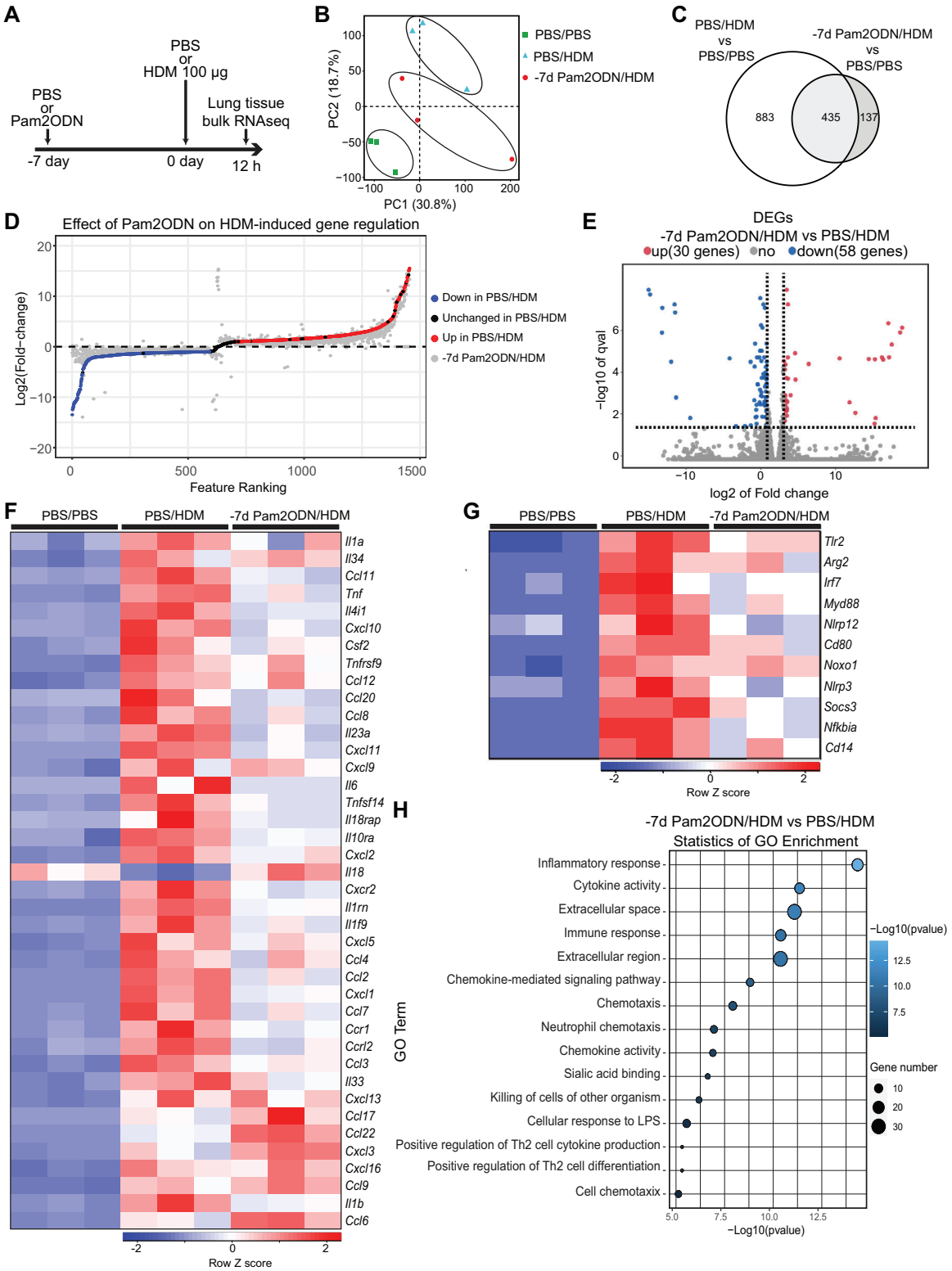

FIGURE 3 | Pam2ODN restricts the expression of HDM-sensitization-induced lung inflammatory transcripts. (A) Experimental design. A single aerosol treatment with PBS or Pam2ODN was administered 7 days before intratracheal sensitization of naïve mice with 100 µg HDM or PBS as a control. Whole lungs were harvested 12 h after the sensitization, and the lung homogenate was prepared for mRNA extraction and subsequent RNA sequencing analysis. (B) Principal component analysis (PCA) showing the gene expression profile in control PBS/PBS compared to PBS- and Pam2ODN-pretreated HDM-sensitized samples. (C) Venn diagram showing the number of genes regulated uniquely in PBS/HDM or Pam2ODN/HDM or shared, relative to the gene expression in control mice PBS/PBS. (D) Ranking plot showing the effect of Pam2ODN pretreatment on HDM-induced genes. HDM-induced upregulated genes are in red, and downregulated genes are in blue. Grey shows the effect of Pam2ODN. (E) Volcano plot of differentially expressed genes (DEGs) (−log10 *q* value and log2 fold change) in Pam2ODN/HDM compared with PBS/HDM. (F) Heatmap showing the relative gene expression

downregulated genes (Figure 4E), genes encoding inflammatory chemokines and cytokines involved in allergic inflammation, such as *Ccl20*, *IL-6, and Csf2*, which encodes GM-CSF, were present (Figure 4E). In contrast, only 30 genes were upregulated in -7d Pam2ODN/HDM and were mostly related to metabolism (*Mttl71a*, *Soat1*, *Dgkh*, *Vldlr*) and immunomodulation (*Pdcd4*, *Ltbp4*, *Mttl71a*) (Figure 4E). Pathway analysis of genes upregulated in -7d Pam2ODN/HDM shows that the top GO biological processes were dominated by lipid metabolic changes related to diacyl glycerol, glycerophospholipid, and phosphatidic acid biosynthetic processes, suggesting that Pam2ODN pretreatment reprograms lipid metabolism towards anabolic over inflammation-associated catabolic metabolism (Figure 4F). On the other hand, the top GO biological processes of genes downregulated in -7d Pam2ODN/HDM were dominated by pathways such as inflammatory response, response to LPS, response to chemokines, and response to bacteria and viruses (Figure 4G). The stringent adjusted *p*-value criterion used in AT2 cell gene analysis prevented the identification of DEGs in airway epithelial cells. Nevertheless, 441 genes, including inflammatory genes like *Isg15*, *Isg20*, *Iftm3*, *JunB*, *IRF7*, *IRF9*, *Cxcl3*, and *Cxcl5* were downregulated in -7d Pam2ODN/HDM mice with raw $p < 0.05$ (Figure S7A). Among the top 10 pathways identified by GO analysis of those downregulated genes are Defense Response to Virus, Response to Cytokines, and Response to Interferon-Beta (Figure S7B). Like in the AT2 cells, the -7d Pam2ODN/HDM mice had fewer upregulated than downregulated genes in airway epithelial cells; most of them were associated with metabolic activities and the control of cell differentiation pathways (Figure S7C). Altogether, these results suggest that Pam2ODN pretreatment has a tolerogenic effect in lung epithelial cells that prevents the HDM sensitization-induced release of inflammatory mediators required for DC recruitment to the lung parenchyma, thereby preventing allergic sensitization.

2.6 | Pam2ODN Imprints Epigenetic Reprogramming in Lung Epithelial Cells

The persistent Pam2ODN effect on airway Th2 polarization and eosinophilic inflammation (Figure 1 and Figure S4) suggests that it induces lung immune tolerance. Unlike adaptive immune memory, trained immunity and tolerance are forms of innate immune memory that are achieved through regulatory epigenetic mechanisms, such as DNA methylation, histone modifications, chromatin accessibility, and noncoding RNA transcription, or through metabolic reprogramming following exposure to a first innate immune stimulus. These mechanisms result in a prolonged state of increased (training) or decreased (tolerance) responsiveness to subsequent inflammatory stimuli such as infection, allergens, air pollutants, or dietary changes [49–52]. To identify epigenetic changes associated with this potential tolerance induced by Pam2ODN against HDM sensitization, we analyzed the chromatin accessibility landscape using scATAC-seq in lung epithelial cells, the first point of contact with both Pam2ODN and HDM allergens [16, 18]. AT1, AT2, and airway epithelial cells were identified in both PBS/HDM and -7d Pam2ODN/HDM mice, with an intriguing shift of AT1 and AT2 populations in the -7d Pam2ODN/HDM mice (Figure 5A). Analysis of differentially accessible chromatin regions (DARs) showed increased chromatin closure and reduced accessibility in AT1 and AT2 cells from Pam2ODN-pretreated mice (Figure 5B,C), reflecting reduced responsiveness to HDM sensitization [53]. Consistent with that observation, for example, in AT1, AT2, and airway epithelial cells of -7d Pam2ODN/HDM mice, we found closed chromatin in the promoter region of *MyD88* (Figure 5D), the lung epithelium driver of HDM-induced Th2 polarization [54], as well as in *Irak1* and *Junb* promoter regions(Figure 5E,F). Chromatin regions of two histone deacetylase (HDAC) molecules, HDAC6 and HDAC8, were similarly closed (Figure 5G,H). While pathways like Interstrand Cross-link Repair and Cellular Response to Oxidative Stress were among the most linked to the accessible DARs (Figure S8C,D), pathway analysis of closed DARs in AT1 and AT2 reveals the restriction of pathways like Polarized Epithelial Cell Differentiation, Cilium Assembly, and Positive Regulation of Catabolic Process (Figure S8A,B). These results suggest that Pam2ODN would be an epigenetic regulator that reprograms lung epithelial cells to prevent HDM-induced inflammatory immune response.

3 | Discussion

In the present study, we investigated how Pam2ODN pretreatment affects the immune interactions between lung epithelial cells and DCs and T cells, thereby preventing lung allergic sensitization and HDM-induced airway eosinophilic inflammation. We show here that inhaled Pam2ODN, prior to HDM sensitization but not after HDM exposure, prevents Th2 polarization of airway CD4+ T cells and eosinophil accumulation following HDM challenge, without affecting the immune responses of Th1, Th17, and Treg cells. This effect lasts for up to 30 days. Although Th1/Th17 immunity also contributes to certain forms of asthma [21], Th2 development in the absence of counterbalancing Th1 immunity, natural killer T cells, or regulatory T cells, which are frequently triggered by infections, has been implicated as a mechanism underlying the rise of allergic sensitization and Th2-mediated lung eosinophilic allergies [55]. Although CpG ODNs have been reported to function as a Th1-inducing adjuvant that skews away from Th2 polarization [56], Pam2ODN reduces HDM-induced airway eosinophils by regulating Th2 cells without counterbalancing effects of Th1 or T regulatory cells. On the other hand, Pam2ODN pretreatment modulates the expression of many genes encoding lung inflammatory cytokines and chemokines, including CCL20, CCL2, GM-CSF, IL-1β, IL-1α, and so on, to prevent the recruitment of proallergic DC2s and moDCs while preserving the population of DC1s at the time of HDM sensitization. DC2s and moDCs respond to epithelia-derived cytokines following allergic sensitization in mice and humans and are required for the antigen presentation and the polarization of CD4+ T cells toward the Th2 phenotype [18, 21]. In contrast, DC1s have a preventive effect against the Th2 immune

of inflammatory cytokines and chemokines genes in PBS/HDM and Pam2ODN/HDM mice relative to their expression in the control PBS/PBS condition. (G) Heatmap showing the relative gene expression of inflammatory signaling and adaptor genes in PBS/HDM and Pam2ODN/HDM mice relative to their expression in control PBS/PBS mice. (H) Gene ontology (GO) term of pathways that are downregulated in Pam2ODN/HDM mice. $N = 3$ mice/group.

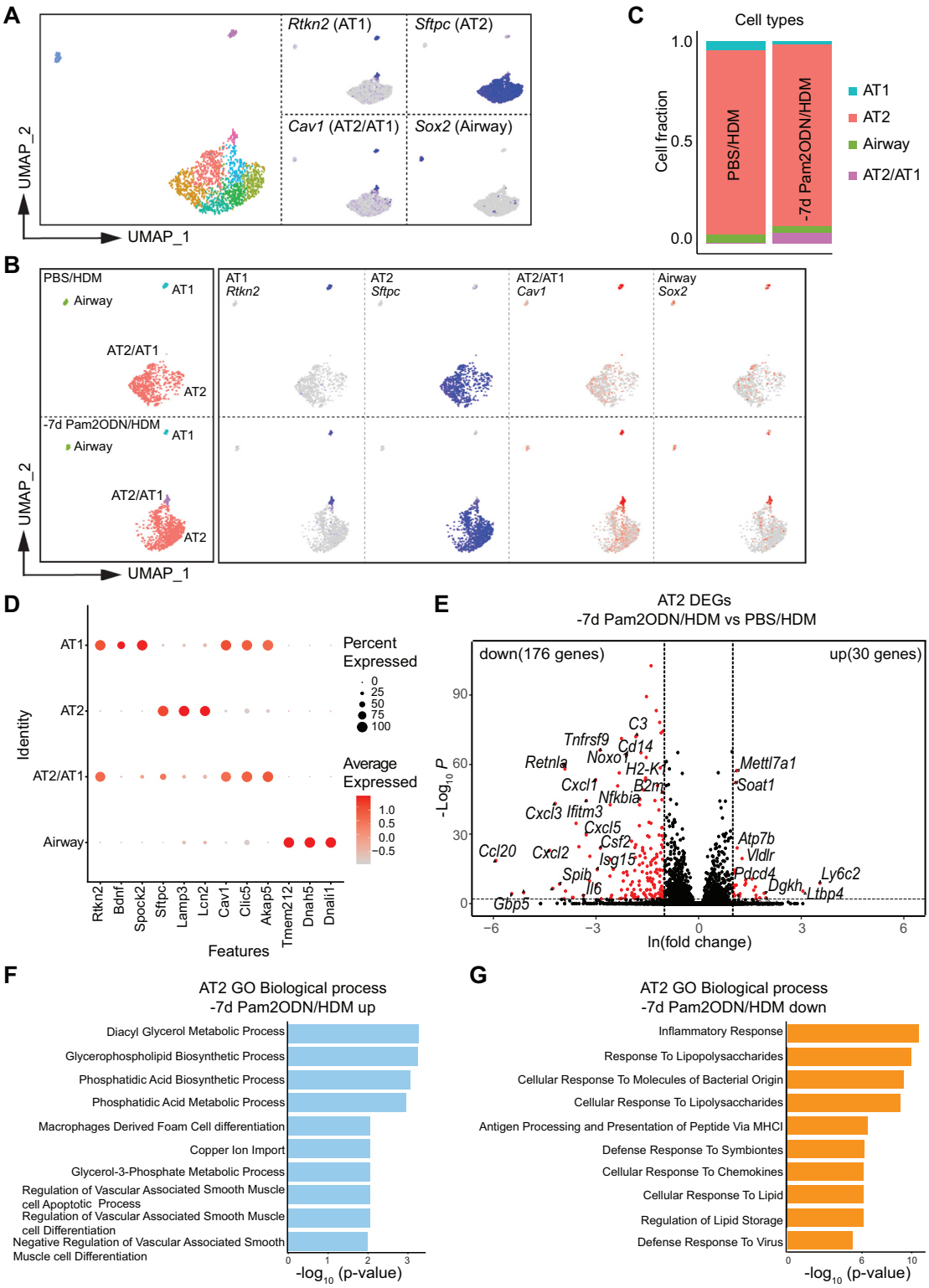

FIGURE 4 | Pam2ODN restricts the expression of inflammatory transcripts induced by HDM sensitization in AT2 cells. A single aerosol treatment with PBS or Pam2ODN was administered 7 days before intratracheal sensitization of naïve mice with 100 μg of HDM. Whole lungs were harvested 12 h after the HDM administration. Lungs were enzymatically digested, and single-cell suspensions were prepared for flow cytometry sorting of the lung epithelial cell population, followed by subsequent single-cell RNA sequencing analysis. (A) UMAP and feature plots of cell types from FACS-purified epithelial cell lineage and their gene markers. (B) UMAP and feature plots showing the remarkable shift of AT2 cell type in the -7d Pam2ODN/HDM mice and the absence of AT2/AT1 transitioning cells in PBS/HDM mice. (C) Summary graph showing fractions of identified cell types in PBS/HDM and -7d Pam2ODN/HDM mice. (D) Dot plot showing canonical markers of identified cell types. (E) Volcano plot of differentially expressed genes (DEGs) in -7d Pam2ODN/HDM compared with PBS/HDM. (F) Gene ontology (GO) term of pathways that are upregulated in -7d Pam2ODN/HDM mice. (G) Gene ontology (GO) term of pathways that are downregulated in -7d Pam2ODN/HDM mice. $N = 3$ mice/group.

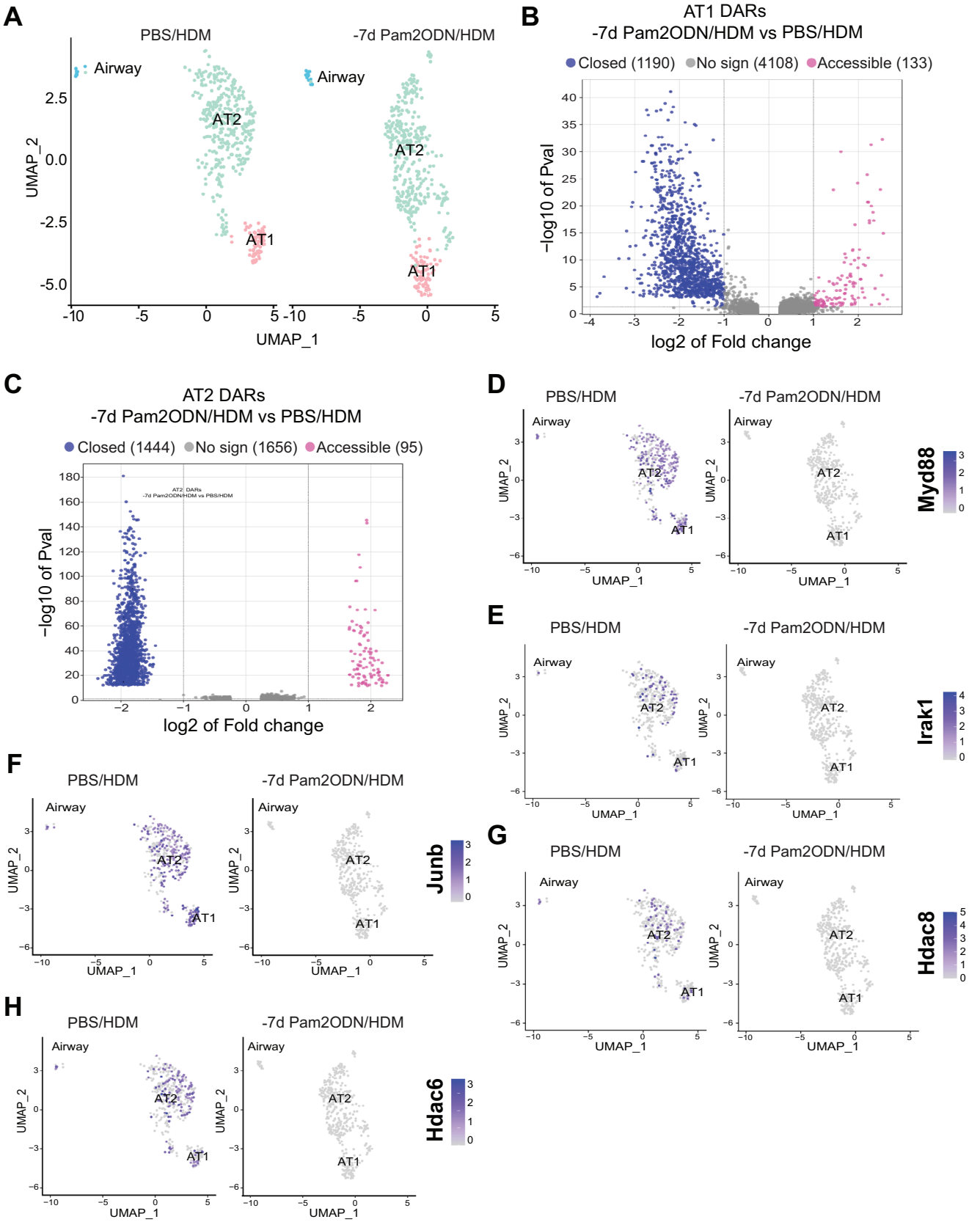

FIGURE 5 | Pam2ODN restricts chromatin accessibility in lung epithelial cells. A single aerosol treatment of PBS or Pam2ODN was administered 7 days before intratracheal sensitization of naïve mice with 100 μg HDM. Whole lungs were harvested 12 h after the HDM administration. Lungs were enzymatically digested, and single-cell suspensions were prepared for flow cytometry sorting of the lung epithelial cell population, followed by subsequent single-cell ATAC sequencing analysis. (A) UMAP plot showing lung epithelial cell populations in PBS-pretreated HDM-sensitized (PBS/HDM) and Pam2ODN-pretreated HDM-sensitized (Pam2ODN/HDM) mice. (B) Volcano plot of differentially accessible chromatin regions

response [39, 40]. Pam2ODN inhibits the activation of DC2s and moDCs to prevent airway Th2 cell polarization and eosinophilic inflammation independently of its effect on other T cell immune responses. While our findings unequivocally demonstrate a link between early suppression of proallergic DCs and a decrease in airway Th2 cells, we will address, in future studies, the specific contributions of DC1s that were preserved in Pam2ODN-treated mice. Interestingly, DC1s have previously been associated with tolerogenic immunity by inducing Treg cells, but Pam2ODN did not alter Treg cell numbers in our study, suggesting alternative mechanisms [39, 40, 57].

Since Pam2ODN pretreatment reduces Th2 cells without inducing compensatory effects on Th1 or T regulatory cells, alternate mechanisms are required to explain the protection.

In addition to being crucial for initiating allergic inflammation, lung epithelial cells coordinate lung innate immunity and control T cell polarization in Type 2 allergic inflammation [18, 20]. HDM extract is contaminated with microbial molecules such as LPS and β-glucan, and it signals through lung epithelial PRRs, such as TLR4 and Dectin-1, to trigger allergic sensitization [4, 5]. Deletion of TLR4 or its downstream adaptor protein MyD88 in lung epithelial cells suppresses allergic sensitization [4, 54]. Using mouse models of asthma, it has been shown that MyD88 expression in epithelial cells is critical for the release of inflammatory mediators that drive the development of Th2-induced eosinophilic inflammation via early recruitment of Th2-polarizing DCs, while MyD88 expression in cDCs, not in epithelial cells, is required for Th17 cell differentiation and the ensuing airway neutrophilia. Therefore, it has been proposed that one way to prevent Th2 cell-induced eosinophilic asthma may be to disrupt MyD88 function in lung epithelial cells [54, 55].

Our RNA-seq data show that MyD88 is inhibited by Pam2ODN pretreatment upon HDM sensitization, which may also account for the suppression of proallergic inflammatory cytokines and pathways. Notably, Pam2ODN suppresses critical pathways of allergic sensitization, including the inflammatory immune response and the LPS response in whole lung and epithelial AT2 cells, consistent with an induction of immunologic tolerance. This finding is in line with data published by Schuijs et al., who showed that pretreatment of lung epithelial cells, in vitro and in vivo, with LPS inhibits sensitization to HDM by suppressing proinflammatory cytokines [55]. However, unlike in their study, Pam2ODN pretreatment did not affect epithelial cell expression of the ubiquitin-modifying enzyme A20, a negative regulator of the transcription factor NF-κB [55].

Pretreatment with Pam2ODN increased the expression of some lipid metabolism pathways. As Pam2ODN protects against bacterial pneumonia in part through epithelial metabolic reprogramming [15], it is plausible that the metabolic alterations seen in -7d Pam2ODN/HDM mice also contribute to protection against lung allergic inflammation. We will investigate this in future studies.

With a protective effect that lasted at least 30 days, we investigated the durability of the tolerogenic effect. Histone modifications, DNA methylation, noncoding RNA transcription, changes in chromatin accessibility, and metabolic reprogramming after exposure to an initial innate immune stimulus are examples of regulatory epigenetic mechanisms that induce immunologic tolerance and trained immunity [49–52]. The decreased epithelial inflammatory gene transcription response to HDM in -7d Pam2ODN/HDM mice prompted us to analyze the chromatin accessibility landscape in lung epithelial cells using scATAC-seq. Consistent with reduced gene transcription seen in our RNA-seq and scRNA-seq in -7d Pam2ODN/HDM mice, the analysis of differentially accessible chromatin regions (DARs) shows increased closed chromatin, which is compatible with reduced transcription [53]. Interestingly, the chromatin region in the MyD88 gene, the key driver of Th2 polarization in lung epithelial cells [54], in AT1, AT2, and airway epithelial cells, was closed in -7d Pam2ODN/HDM mice. Similarly, IRAK1, which is recruited to the receptor-signaling complex by MyD88 upon TLR activation, leading to the activation of downstream signaling pathways such as inflammatory NF-κB [58], also had its chromatin region closed. Moreover, thymoquinone, an IRAK1 antagonist, inhibits Type 2 allergic inflammation in the murine asthma model [59, 60]. The chromatin region in the MyD88 downstream AP-1-associated transcription factor JunB was also closed [61, 62]. Transcription factor JunB drives T cell expression of Type 2 inflammatory cytokines [63]. Thus, our data support the idea that Pam2ODN imprinting induces a MyD88-mediated tolerogenic effect.

Histone acetylation and methylation control the activation state of both inflammatory and anti-inflammatory genes [49, 64]. Chromatin regions of two HDAC molecules, HDAC6 and HDAC8, were closed in lung epithelial cells from -7d Pam2ODN/HDM mice. Of the 18 HDACs identified in mammals [65], HDAC6 is of particular interest in inflammatory diseases. Notably, specific inhibition of HDAC6 with ACY-1215 or inhibition of Class I and II HDACs with SAHA in LPS-activated RAW264.7 cells attenuates LPS-TLR4 signaling and reduces the overproduction of ROS and the expression of pro-inflammatory cytokines like TNF-α, IL-1β, and IL-6, which are downstream of MyD88 [66–69]. MyD88 is also a target of HDAC6 in lung endothelial cells [70]. This suggests that Pam2ODN may modify histone acetylation pathways in lung epithelial cells to inhibit the expression of genes associated with inflammation.

Here, we demonstrated that, without rebalancing Th1, Th17, or Treg immunological responses, Pam2ODN has a long-lasting preventive impact against the development of Th2-induced lung eosinophilic allergic inflammation. This tolerogenic impact is linked to a significant reprogramming of the lung's epithelium, which includes immunomodulation of the TLR-MyD88 pathway. Thus, Pam2ODN, which is well tolerated in humans (NCT04313023, NCT04312997, NCT03794557, NCT02566252, NCT02124278), is a promising candidate as a

(DARs) in AT1 and (C) AT2 -7d Pam2ODN/HDM relative to PBS/HDM treatment condition. (D-H) Feature plots showing chromatin accessibility in (D) MyD88, (E) Irak1, (F) JunB, (G) Hdac6, and (H) Hdac8 of lung epithelial cell populations in PBS-pretreated HDM-sensitized (PBS/HDM) and Pam2ODN-pretreated HDM-sensitized (Pam2ODN/HDM) mice. $N = 3$ mice/group.

means of mitigating allergic sensitization and, potentially, as a strategy to mitigate the rise in allergic lung diseases.

4 | Data Limitations and Perspectives

That Pam2ODN only confers protection against HDM prior to sensitization is a notable limitation of this strategy in its clinical translation, as it would be challenging for clinicians to treat infants with Pam2ODN before exposure to HDM universally. However, this limitation is not observed for Pam2ODN-induced protection against other forms of allergic inflammation in the lungs, such as Sendai virus-induced asthma. Further, antimicrobial protection can be induced by Pam2ODN after pathogen exposure, particularly against lethal viral infections. Thus, although it may not be immediately practical to deliver Pam2ODN to all pre-HDM-exposed infants, the current studies with HDM may provide mechanistic insights into why Pam2ODN protects against different allergic exposures at varying time points. In addition, since a large percentage of clinical asthma exacerbations are induced by viral infections, the effect of Pam2ODN on both allergic immunomodulation and antiviral defense may have a synergistic benefit in reducing asthma exacerbations and progression.

5 | Material and Methods

5.1 | Mice

Wild-type breeder BALB/cJ mice were obtained from the Jackson Laboratory (Sacramento, CA) and housed in specific pathogen-free conditions on a 12-h light/dark cycle with unrestricted access to food and water. Mice were euthanized by intraperitoneal injection of 2,2,2-tribromoethanol (250 mg/kg) and exsanguinated by transection of the abdominal aorta. Unless otherwise noted, every cohort of mice used in these studies was female. Each experiment was conducted at least three times, except for all the transcriptomic analyses. Every procedure was carried out in compliance with the Texas A&M Institute for Biosciences and Technology's and MD Anderson Cancer Center's Institutional Animal Care and Use Committee. Unless otherwise specified, chemicals were purchased from Sigma-Aldrich (St. Louis, MO).

5.2 | Treatment With Aerosolized Pam2ODN

This was performed as previously described [71]. Briefly, we purchased 2,3-bis(palmitoyloxy)-2-propyl-Cys-Ser-Lys-Lys-Lys-Lys-OH (Pam2CSK4) as the trifluoroacetic acid salt from Bachem and oligodeoxynucleotide 5′ TCG TCG TCG TTC GAA CGA CGT TGA T 3′ as the sodium salt on a nuclease-resistant phosphorothioate backbone (ODN M362) from TriLink BioTechnologies. A solution of ODN (1 μM) and Pam2CSK4 (4 μM) in 8 mL of endotoxin-free sterile PBS was placed in an Aerotech II nebulizer (Biodex Medical Systems, Shirley, NY) driven by 10 L/min of 5% CO2 in air to promote deep breathing. Polyethylene tubing (30 cm × 22 mm) was used to connect the nebulizer to a 10-L polyethylene container that was vented to a biosafety hood. Mice were exposed to the aerosol for ~40 min. The optimal molar ratio between Pam2 and ODN was previously determined [72]. The Pam2ODN dose was chosen to reflect the upper shoulder of the dose-response curves for secreted epithelial cytokines, leukocyte recruitment, and antimicrobial efficacy [71]. In all the study's experiments, the dosage, method, and general procedure for giving a Pam2ODN therapy were identical.

5.3 | Sensitization and Airway Challenge With HDM

Lyophilized HDM extract (Stallergenes Greer, Lenoir, NC) was reconstituted in PBS. As previously described [16], mice were suspended by their upper incisors on a board at a 60° angle from horizontal while under isoflurane anesthesia, then were sensitized to 100 μg of HDM (protein weight) by depositing 40 μL of reconstituted HDM into the oropharynx and permitting aspiration into the lungs. In some experiments, mice were challenged with 10 μg of HDM by depositing the same volume of reconstituted HDM into the nasal vestibule. The mice in all experiments were 7–10 weeks old at the time of HDM sensitization.

5.4 | Bronchoalveolar Lavage Collection

This was performed as previously, with slight modifications [71]. We instilled and collected 1 mL of ice-cold PBS 5% FBS four times from each mouse through a 20-gauge cannula inserted through rings of the exposed trachea of euthanized animals. The collection was spun down at 1500 rpm at 4°C. Red blood cells were lysed with the addition of 1 mL of red blood cell lysis buffer (15 mM NH_4Cl, 12 mM $NaHCO_3$, 0.1 mM EDTA, pH 8.0). After samples were incubated on ice for 3 min with red blood cell lysis buffer, cells were washed with PBS and resuspended in FACS staining buffer (PBS supplemented with 1% FBS) before staining for specific cell types.

5.5 | Lung Single-Cell Suspension Preparation for Flow Cytometry

As previously described with slight modifications [71], mouse lungs were perfused with 5–10 mL PBS, dissected, cut into 1 mm^3 pieces, and digested with collagenase/DNAse I (5 mg/mL, Worthington Biochemical) for 30–45 min at 37°C. After digestion, single cells were collected by passing through a 70 μm filter (Falcon, 352350) and washed one time with PBS. Red blood cells were lysed with 1 mL of red blood cell lysis buffer (15 mM NH_4Cl, 12 mM $NaHCO_3$, 0.1 mM EDTA, pH 8.0), and the samples were incubated on ice for 3 min. These single cells were washed with PBS and resuspended in FACS staining buffer before staining for specific cell types.

5.6 | Flow Cytometry

Single cells from disaggregated lungs and mediastinal lymph nodes, or BAL fluid, were incubated with a specific monoclonal antibody against CD16/CD32 (Biolegend, clone 93) to block Fc receptors before surface staining. The antibodies used for cell surface labeling were RedFluor anti-CD45 (TONBO biosciences,

30-F11), PercPcy5.5 anti-CD3 (TONBO biosciences, 145-2C11), PEcy7 anti-CD4 (TONBO biosciences, RM4-5), PercPcy5.5 anti-CD11b (eBiosciences, M1/70), BV421 anti-mouse Lineage cocktail (Biolegend, 17A2; RB6-8C5; RA3-6B2; Ter-119; M1/70), BUV737 anti-CD11c (BD Biosciences, N418), PEcy7 anti-MHCII (Biolegend, M5/114.15.2), BV650 anti-Ly6C (Biolegend, HK1.4), PE anti-Ly6G (Biolegend, 1A8), BV711 anti-CD64 (Biolegend, X54.5/7.1), PE-CF594 anti-Siglec-F (BD Biosciences, E50-2440), FITC anti-F4/80 (eBiosciences, BM8), and BV785 anti-CD103 (Biolegend, 2E7). To exclude dead cells, Live/Dead UV450 (TONBO Biosciences) was added to the antibody cocktail. For intracellular staining of transcription factors, cells were washed two times with the staining buffer after the surface staining, fixed and permeabilized using Cytofix/Cytoperm buffer (eBioscience), then stained with AF488 anti-Gata3 (eBiosciences, TWAJ), BV785 anti-Tbet (Biolegend, 4B10), PE anti-RORγt (BD Biosciences, Q21-559), and AF647 anti-Foxp3 (Biolegend, QA 20A67) mAb, washed two times with permeabilization buffer (eBioscience), fixed with 2% formaldehyde, acquired, and analyzed using a BD LSRFortessa X-20 instrument (BD Biosciences) and the FlowJo software (Tree Star, Ashland, OR, USA), respectively.

5.7 | ELISA of Cytokines in BALF

Mice were anesthetized, and bronchoalveolar lavage was performed twice using 1 mL of PBS containing 1% FBS. The recovered BALF was combined and centrifuged at 1500 rpm for 5 min at 4°C. The cell-free BALF was used to quantify IL-5, IL-13, IL-10, IL-17A, and IFN-γ using the corresponding ELISA kits (Proteintech, USA) according to the manufacturer's instructions.

5.8 | RNA Extraction

After euthanasia as described above, the thoracic cavity was dissected, lungs were removed after PBS perfusion via the heart and subsequently placed in a 15 mL test tube containing 5 mL RNAlater (Millipore Sigma). Lungs were weighed and homogenized in RNAlater until smooth using a bead beater. RNA was isolated from lungs using Qiagen RNeasy mini kits (Qiagen, CA, USA) according to the manufacturer's instructions, then submitted for RNA sequencing.

5.9 | RNA Sequencing

RNA-seq was performed at LC Sciences (Houston, Texas). A poly (A) RNA sequencing library was prepared following Illumina's TruSeq-stranded-mRNA sample preparation protocol. An Agilent Technologies 2100 Bioanalyzer was used to verify the integrity of the RNA. Oligo-(dT) magnetic beads were used to purify poly (A) tail-containing mRNAs in two rounds. Following purification, a divalent cation buffer was used to denature poly (A) RNA at high temperature. With the Agilent Technologies 2100 Bioanalyzer High Sensitivity DNA Chip, the sequencing library was quantified and subjected to quality control analysis. Illumina's NovaSeq 6000 sequencing machine was used to carry out paired-ended sequencing. For the Transcripts Assembly, first, readings containing adaptor contamination, low-quality bases, and unknown bases were eliminated using Cutadapt [73] and in-house Perl scripts.

Next, FastQC (http://www.bioinformatics.babraham.ac.uk/projects/fastqc/) was used to confirm the quality of the sequence. To map the reads to the genome at ftp.ensembl.org/pub/release-101/fasta/mus_musculus/dna/, we used HISAT2 [74]. The mapped reads of each sample were assembled using StringTie [75]. A comprehensive transcriptome was then created by combining all transcriptomes using Perl scripts and gffcompare. After the final transcriptome was created, Ballgown (http://www.bioconductor.org/packages/release/bioc/html/ballgown.html) and StringTie were used to estimate the expression levels of each transcript [75]. For the Differential expression analysis of mRNAs, StringTie [75] was used to calculate FPKM. R package DESeq2 [76] and R package edgeR [77] were used to analyze the differences in mRNA expression between two groups and two samples, respectively. Differentially expressed mRNAs were defined as those whose absolute fold change was ≥ 2 and whose false discovery rate (FDR) was less than 0.05. Raw data have been deposited in GEO under the accession number GSE299556.

5.10 | Lung Dissociation and Flow Cytometry Cell-Sorting

This was performed as previously described with minor modifications [78]. After being dissected in PBS and cut into pieces using forceps, the entire lung was digested in 1 mL Liebovitz media (Gibco, 21083-027) for 30 min at 37°C with 0.5 mg/mL of DNase I (Worthington, D, LS002007), 2 mg/mL of collagenase Type I (Worthington, CLS-1, LS004197), and 2 mg/mL of elastase (Worthington, ESL, LS002294). By pipetting up and down, a mechanical trituration was performed on the tissue at 15 min during digestion until the piece was small enough to pass through the pipette tip. Following the addition of 20% fetal bovine serum, 300 µL (FBS, Invitrogen, 10082–139) to stop the enzymatic reaction, the tissue was homogenized by trituration. The samples were put on ice in the cold room, filtered through a 70 µm cell strainer (Falcon, 352350), and spun down for one minute at 5000 rpm. This was followed by the removal of the supernatant, the addition of 1 mL of red blood cell lysis buffer (15 mM NH_4Cl, 12 mM $NaHCO_3$, 0.1 mM EDTA, pH 8.0), and incubation of the samples on ice for 3 min. Cells were pelleted again by centrifugation at 5000 × *g* for 1 min, washed with Liebovitz + 10% FBS, resuspended with 1 mL Liebovitz + 10% FBS, and filtered through a 70 µm cell strainer into a 5 mL glass tube. Samples were stained with CD45-PE/Cy7 (BioLegend, 103114), ECAD-PE (BioLegend, 147304), and ICAM2-A647 (Invitrogen, A15452) antibodies (1:250 dilutions for all antibodies) for 30 min on ice. SYTOX Blue (1:1000, Invitrogen, S34857) was added for viability. A BD FACS Aria Fusion Cell Sorter was used to sort the samples. Dead cells and doublets were excluded. For scRNA-seq and scATAC-seq, the $CD45^{-}ICAM2^{-}ECAD^{+}$ cells were collected as the epithelial cell lineage (extended Figure S6A) and submitted for library preparation using the 10× Genomics platform.

5.11 | Single-Cell RNA Sequencing

Cells sorted from 8-week-old mice, as mentioned above, were processed using the 3′ Library and Gel Bead Kit in accordance with the Chromium Single-Cell Gene Expression Solution Platform (10× Genomics) user manual (v2 rev D). The scRNA-seq for the PBS/HDM and -7d Pam2ODN/HDM samples were processed using the 3′ Library and Gel Bead Kit following the manufacturer's user guide (v3 rev D). The Illumina NextSeq500 or NovaSeq6000 was then used to sequence all libraries in a 26 × 124 format with an 8 bp index (Read1). PBS/HDM versus -7d Pam2ODN/HDM were merged using Cell Ranger's "cellranger count" and "cellranger aggr." The Seurat R package (v3) [79] and custom R scripts were used for downstream analysis. Cells that had fewer than 200 genes or more than 5000 genes were filtered out. The epithelial lineage cluster was identified using the Cdh1 marker as previously published [80]. Epithelial cell types were identified using Rtkn2 for Type 1 alveolar epithelial cells, Sftpc for Type 2 alveolar epithelial cells, Cav1 for AT2/AT1 transitioning alveolar epithelial cells, and Sox2 for airway epithelial cells. Model-based analysis of single-cell transcriptomics (MAST) was used to identify DEGs [81]. -7d Pam2ODN/HDM and PBS/HDM samples were processed in parallel experimentally and computationally and thus spatially comparable in the UMAP plots. Raw data have been deposited in GEO under the accession number GSE299705.

5.12 | Single-Cell ATAC Sequencing

Lung epithelial cells were sorted from 8-week-old mice and processed using the 10× Genomics Chromium Single Cell ATAC platform with the 3′ Library and Gel Bead Kit, following the manufacturer's protocol. Libraries were sequenced on an Illumina NovaSeq 6000 system using 50 bp paired-end reads, with Indexes 1 and 2 sequenced for 8 and 16 cycles, respectively. Raw sequencing data were processed using the cellranger-atac count function in the Cell Ranger ATAC pipeline to generate fragment files and peak-barcode matrices. Downstream analysis was performed in R using the Seurat (version 4.3) and Signac (version 1.9) packages (https://github.com/timoast/signac), along with custom scripts. Cells were filtered based on quality control criteria: unique peak counts greater than 100,000 or fewer than 1000, less than 25% of reads in peaks, blacklist ratio greater than 0.025, nucleosome signal score above 10, or transcription start site (TSS) enrichment score below 2. Gene activity scores were computed using a ± 2 kb window around TSSs. Cell types were assigned based on marker gene activity: Spock2 for alveolar Type 1 (AT1), Lamp3 for alveolar Type 2 (AT2), and Sox2 for airway epithelial cells. Raw data have been deposited in GEO under the accession number GSE299558.

5.13 | Statistical Analysis

Data are displayed as means ± standard deviations of the mean for the numbers of mice, as indicated. Statistics were performed by GraphPad Prism using one-way ANOVA with Bartlett's test correction for multiple comparisons. $p < 0.05$ was considered statistically significant.

Author Contributions

M.N. designed and performed the experiments, analyzed the data, created the figures, and wrote the manuscript. C.S.L.K., D.H., and J.P.G. analyzed the data, created the figures, and wrote the manuscript. R.N. and Y.W. performed the experiments. J.C. and S.E.E. provided funding. S.E.E. conceptualized the project, designed experiments, provided critical evaluation of data, and edited the manuscript.

Acknowledgments

Scott E. Evans acknowledges grants R35 HL144805 and DP2 HL123229; Jichao Chen acknowledges grants R01HL130129 and R01HL153511. MN was a University of Texas MD Anderson Cancer Center Postdoctoral Research Fellow. The MD Anderson Advanced Genomics Technology Core is supported by a core grant CA016672. The Flow Cytometry and Cellular Imaging Core Facility was supported in part by The University of Texas MD Anderson Cancer Center and P30CA016672.

Ethics Statement

The animal study was reviewed and approved by the IACUC, MD Anderson Cancer Center.

Conflicts of Interest

Scott E. Evans is the inventor of US patent 8,883,174 "Compositions for Stimulation of Mammalian Innate Immune Resistance to Pathogens," which has been licensed by their employer, the University of Texas MD Anderson Cancer Center, to Pulmotect, Inc., which is developing Pam2ODN as a therapeutic for respiratory infections. The other authors declare no conflicts of interest.

Data Availability Statement

The raw data supporting the conclusion of this article will be made available by the authors, without undue reservation. RNA-seq, scRNA-seq, and scATAC-seq raw data have been deposited in GEO under the accession numbers GSE299556, GSE299705, and GSE299558, respectively.

Peer Review

The peer review history for this article is available at https://publons.com/publon/10.1002/eji.70172.

References

1. L. B. Murrison, E. B. Brandt, J. B. Myers, and G. K. K. Hershey, "Environmental Exposures and Mechanisms in Allergy and Asthma Development," *Journal of Clinical Investigation* 129, no. 4: 1504–1515, https://doi.org/10.1172/JCI124612.

2. L. A. Reynolds and B. B. Finlay, "Early Life Factors That Affect Allergy Development," *Nature Reviews Immunology* 17, no. 8 (2017): 518–528, https://doi.org/10.1038/nri.2017.39.

3. M. M. Stein, C. L. Hrusch, J. Gozdz, et al., "Innate Immunity and Asthma Risk in Amish and Hutterite Farm Children," *New England Journal of Medicine* 375, no. 5 (2016): 411–421, https://doi.org/10.1056/NEJMoa1508749.

4. H. Hammad, M. Chieppa, F. Perros, M. A. Willart, R. N. Germain, and B. N. Lambrecht, "House Dust Mite Allergen Induces Asthma via Toll-Like Receptor 4 Triggering of Airway Structural Cells," *Nature Medicine* 15, no. 4 (2009): 410–416, https://doi.org/10.1038/nm.1946.

5. A. T. Nathan, E. A. Peterson, J. Chakir, and M. Wills-Karp, "Innate Immune Responses of Airway Epithelium to House Dust Mite Are Mediated Through β-Glucan–Dependent Pathways," *Journal of Allergy and Clinical Immunology* 123, no. 3 (2009): 612–618, https://doi.org/10.1016/j.jaci.2008.12.006.

6. C. E. Whetstone, M. Ranjbar, H. Omer, R. P. Cusack, and G. M. Gauvreau, "The Role of Airway Epithelial Cell Alarmins in Asthma," *Cells* 11, no. 7 (2022): 1105, https://doi.org/10.3390/cells11071105.

7. I. Morianos and M. Semitekolou, "Dendritic Cells: Critical Regulators of Allergic Asthma," *International Journal of Molecular Sciences* 21, no. 21 (2020): 7930, https://doi.org/10.3390/ijms21217930.

8. B. N. Lambrecht and H. Hammad, "Biology of Lung Dendritic Cells at the Origin of Asthma," *Immunity* 31, no. 3 (2009): 412–424, https://doi.org/10.1016/j.immuni.2009.08.008.

9. C. M. Lloyd and E. M. Hessel, "Functions of T Cells in Asthma: More Than Just TH2 Cells," *Nature Reviews Immunology* 10, no. 12 (2010): 838–848, https://doi.org/10.1038/nri2870.

10. M. C. Peters, L. Ringel, N. Dyjack, et al., "A Transcriptomic Method to Determine Airway Immune Dysfunction in T2-High and T2-Low Asthma," *American Journal of Respiratory and Critical Care Medicine* 199, no. 4 (2019): 465–477, https://doi.org/10.1164/rccm.201807-1291OC.

11. D. S. Robinson, Q. Hamid, S. Ying, et al., "Predominant TH2-Like Bronchoalveolar T-Lymphocyte Population in Atopic Asthma," *New England Journal of Medicine* 326, no. 5 (1992): 298–304, https://doi.org/10.1056/NEJM199201303260504.

12. C. A. Tibbitt, J. M. Stark, L. Martens, et al., "Single-Cell RNA Sequencing of the T Helper Cell Response to House Dust Mites Defines a Distinct Gene Expression Signature in Airway Th2 Cells," *Immunity* 51, no. 1 (2019): 169–184.e5, https://doi.org/10.1016/j.immuni.2019.05.014.

13. D. L. Goldblatt, J. R. Flores, G. Valverde Ha, et al., "Inducible Epithelial Resistance Against Acute Sendai Virus Infection Prevents Chronic Asthma-Like Lung Disease in Mice," *British Journal of Pharmacology* 177, no. 10 (2020): 2256–2273, https://doi.org/10.1111/bph.14977.

14. Y. Wang, V. V. Kulkarni, J. PantaleónGarcía, et al., "The RNA Receptor RIG-I Binding Synthetic Oligodeoxynucleotide Promotes Pneumonia Survival," *JCI Insight* 9, no. 21 (2024): e180584, https://doi.org/10.1172/jci.insight.180584.

15. Y. Wang, V. V. Kulkarni, J. P. García, et al., "Antimicrobial Mitochondrial Reactive Oxygen Species Induction by Lung Epithelial Immunometabolic Modulation," *PLOS Pathogens* 19, no. 9 (2023): e1011138, https://doi.org/10.1371/journal.ppat.1011138.

16. D. L. Goldblatt, G. Valverde Ha, S. Wali, et al., "Epithelial Immunomodulation by Aerosolized Toll-Like Receptor Agonists Prevents Allergic Inflammation in Airway Mucosa in Mice," *Frontiers in Pharmacology* 13 (2022): 833380, https://doi.org/10.3389/fphar.2022.833380.

17. J. A. Whitsett and T. Alenghat, "Respiratory Epithelial Cells Orchestrate Pulmonary Innate Immunity," *Nature Immunology* 16, no. 1 (2015): 27–35, https://doi.org/10.1038/ni.3045.

18. S. Lameire and H. Hammad, "Lung Epithelial Cells: Upstream Targets in Type 2-High Asthma," *European Journal of Immunology* 53, no. 11 (2023): e2250106, https://doi.org/10.1002/eji.202250106.

19. C. Doras, F. Petak, S. Bayat, et al., "Lung Responses in Murine Models of Experimental Asthma: Value of House Dust Mite Over Ovalbumin Sensitization," *Respiratory Physiology & Neurobiology* 247 (2018): 43–51, https://doi.org/10.1016/j.resp.2017.09.001.

20. H. Hammad and B. N. Lambrecht, "The Basic Immunology of Asthma," *Cell* 184, no. 6 (2021): 1469–1485, https://doi.org/10.1016/j.cell.2021.02.016.

21. B. N. Lambrecht and H. Hammad, "The Immunology of Asthma," *Nature Immunology* 16, no. 1 (2015): 45–56, https://doi.org/10.1038/ni.3049.

22. A. Schnell, D. R. Littman, and V. K. Kuchroo, "TH17 cell Heterogeneity and Its Role in Tissue Inflammation," *Nature Immunology* 24, no. 1 (2023): 19–29, https://doi.org/10.1038/s41590-022-01387-9.

23. J. A. Hall, M. Pokrovskii, L. Kroehling, et al., "Transcription Factor RORα Enforces Stability of the Th17 Cell Effector Program by Binding to a Rorc Cis-Regulatory Element," *Immunity* 55, no. 11 (2022): 2027–2043.e9, https://doi.org/10.1016/j.immuni.2022.09.013.

24. Y. Xie, P. W. Abel, T. B. Casale, and Y. Tu, "T Helper 17 Cells and Corticosteroid Insensitivity in Severe Asthma," *Journal of Allergy and Clinical Immunology* 149, no. 2 (2022): 467–479, https://doi.org/10.1016/j.jaci.2021.12.769.

25. A. Ray and J. K. Kolls, "Neutrophilic Inflammation in Asthma and Association With Disease Severity," *Trends in Immunology* 38, no. 12 (2017): 942–954, https://doi.org/10.1016/j.it.2017.07.003.

26. G. Izumi, H. Nakano, K. Nakano, et al., "CD11b+ Lung Dendritic Cells at Different Stages of Maturation Induce Th17 or Th2 Differentiation," *Nature Communications* 12, no. 1 (2021): 5029, https://doi.org/10.1038/s41467-021-25307-x.

27. S. J. Szabo, S. T. Kim, G. L. Costa, X. Zhang, C. G. Fathman, and L. H. Glimcher, "A Novel Transcription Factor, T-Bet, Directs Th1 Lineage Commitment," *Cell* 100, no. 6 (2000): 655–669, https://doi.org/10.1016/S0092-8674(00)80702-3.

28. J. D. Fontenot, M. A. Gavin, and A. Y. Rudensky, "Foxp3 Programs the Development and Function of CD4+CD25+ Regulatory T Cells," *Nature Immunology* 4, no. 4 (2003): 330–336, https://doi.org/10.1038/ni904.

29. S. Hori, T. Nomura, and S. Sakaguchi, "Control of Regulatory T Cell Development by the Transcription Factor Foxp3," *Science* 299, no. 5609 (2003): 1057–1061, https://doi.org/10.1126/science.1079490.

30. A. Chaudhry, R. M. Samstein, P. Treuting, et al., "Interleukin-10 Signaling in Regulatory T Cells Is Required for Suppression of Th17 Cell-Mediated Inflammation," *Immunity* 34, no. 4 (2011): 566–578, https://doi.org/10.1016/j.immuni.2011.03.018.

31. J. D. Campbell, K. F. Buckland, S. J. McMillan, et al., "Peptide Immunotherapy in Allergic Asthma Generates IL-10–Dependent Immunological Tolerance Associated With Linked Epitope Suppression," *Journal of Experimental Medicine* 206, no. 7 (2009): 1535–1547, https://doi.org/10.1084/jem.20082901.

32. M. Ostroukhova, Z. Qi, T. B. Oriss, B. Dixon-McCarthy, P. Ray, and A. Ray, "Treg-Mediated Immunosuppression Involves Activation of the Notch-HES1 Axis by Membrane-Bound TGF-β," *Journal of Clinical Investigation* 116, no. 4 (2006): 996–1004, https://doi.org/10.1172/JCI26490.

33. A. M. Bilate and J. J. Lafaille, "Induced CD4+Foxp3+ Regulatory T Cells in Immune Tolerance," *Annual Review of Immunology* 30 (2012): 733–758, https://doi.org/10.1146/annurev-immunol-020711-075043.

34. M. Plantinga, M. Guilliams, M. Vanheerswynghels, et al., "Conventional and Monocyte-Derived CD11b (+) Dendritic Cells Initiate and Maintain T Helper 2 Cell-Mediated Immunity to House Dust Mite Allergen," *Immunity* 38, no. 2 (2013): 322–335, https://doi.org/10.1016/j.immuni.2012.10.016.

35. K. Furuhashi, T. Suda, H. Hasegawa, et al., "Mouse Lung CD103+ and CD11b High Dendritic Cells Preferentially Induce Distinct CD4+ T-Cell Responses," *American Journal of Respiratory Cell and Molecular Biology* 46, no. 2 (2012): 165–172, https://doi.org/10.1165/rcmb.2011-0070OC.

36. J. Deckers, D. Sichien, M. Plantinga, et al., "Epicutaneous Sensitization to House Dust Mite Allergen Requires Interferon Regulatory Factor 4-Dependent Dermal Dendritic Cells," *Journal of Allergy and Clinical Immunology* 140, no. 5 (2017): 1364–1377.e2, https://doi.org/10.1016/j.jaci.2016.12.970.

37. D. Sichien, C. L. Scott, L. Martens, et al., "IRF8 Transcription Factor Controls Survival and Function of Terminally Differentiated Conventional and Plasmacytoid Dendritic Cells, Respectively," *Immunity* 45, no. 3 (2016): 626–640, https://doi.org/10.1016/j.immuni.2016.08.013.

38. G. E. Grajales-Reyes, A. Iwata, J. Albring, et al., "Batf3 Maintains Autoactivation of Irf8 for Commitment of a CD8α (+) Conventional DC Clonogenic Progenitor," *Nature Immunology* 16, no. 7 (2015): 708–717, https://doi.org/10.1038/ni.3197.

39. L. Conejero, S. C. Khouili, S. Martínez-Cano, H. M. Izquierdo, P. Brandi, and D. Sancho, "Lung CD103+ Dendritic Cells Restrain Allergic

Airway Inflammation Through IL-12 Production," *JCI Insight* 2, no. 10 (2017): e90420, https://doi.org/10.1172/jci.insight.90420.

40. J. L. Coombes, K. R. R. Siddiqui, C. V. Arancibia-Cárcamo, et al., "A Functionally Specialized Population of Mucosal CD103+ DCs Induces Foxp3+ Regulatory T Cells via a TGF-Beta and Retinoic Acid-Dependent Mechanism," *Journal of Experimental Medicine* 204, no. 8 (2007): 1757–1764, https://doi.org/10.1084/jem.20070590.

41. G. H. Hong, H. S. Kwon, K. A. Moon, et al., "Clusterin Modulates Allergic Airway Inflammation by Attenuating CCL20-Mediated Dendritic Cell Recruitment," *Journal of Immunology* 196, no. 5 (2016): 2021–2030, https://doi.org/10.4049/jimmunol.1500747.

42. H. Hammad and B. N. Lambrecht, "Barrier Epithelial Cells and the Control of Type 2 Immunity," *Immunity* 43, no. 1 (2015): 29–40, https://doi.org/10.1016/j.immuni.2015.07.007.

43. B. N. Lambrecht, H. Hammad, and J. V. Fahy, "The Cytokines of Asthma," *Immunity* 50, no. 4 (2019): 975–991, https://doi.org/10.1016/j.immuni.2019.03.018.

44. T. Zhu, A. P. Brown, L. P. Cai, G. Quon, and H. Ji, "Single-Cell RNA-Seq Analysis Reveals Lung Epithelial Cell Type-Specific Responses to HDM and Regulation by Tet1," *Genes* 13, no. 5 (2022): 880, https://doi.org/10.3390/genes13050880.

45. A. M. Olajuyin, X. Zhang, and H. L. Ji, "Alveolar Type 2 Progenitor Cells for Lung Injury Repair," *Cell Death Discovery* 5, no. 1 (2019): 1–11, https://doi.org/10.1038/s41420-019-0147-9.

46. M. Chan and Y. Liu, "Function of Epithelial Stem Cell in the Repair of Alveolar Injury," *Stem Cell Research & Therapy* 13 (2022): 170, https://doi.org/10.1186/s13287-022-02847-7.

47. C. Klaßen, A. Karabinskaya, L. Dejager, et al., "Airway Epithelial Cells Are Crucial Targets of Glucocorticoids in a Mouse Model of Allergic Asthma," *Journal of Immunology* 199, no. 1 (2017): 48–61, https://doi.org/10.4049/jimmunol.1601691.

48. D. C. Do, Y. Zhang, W. Tu, et al., "Type II Alveolar Epithelial Cell-Specific Loss of RhoA Exacerbates Allergic Airway Inflammation Through SLC26A4," *JCI Insight* 6, no. 14 (2021): e148147, https://doi.org/10.1172/jci.insight.148147.

49. D. C. Ifrim, J. Quintin, L. A. B. Joosten, et al., "Trained Immunity or Tolerance: Opposing Functional Programs Induced in Human Monocytes After Engagement of Various Pattern Recognition Receptors," *Clinical and Vaccine Immunology* 21, no. 4 (2014): 534–545, https://doi.org/10.1128/CVI.00688-13.

50. M. Wegmann, "Trained Immunity in Allergic Asthma," *Journal of Allergy and Clinical Immunology* 151, no. 6 (2023): 1471–1473, https://doi.org/10.1016/j.jaci.2023.02.023.

51. S. Fanucchi, J. Domínguez-Andrés, L. A. B. Joosten, M. G. Netea, and M. M. Mhlanga, "The Intersection of Epigenetics and Metabolism in Trained Immunity," *Immunity* 54, no. 1 (2021): 32–43, https://doi.org/10.1016/j.immuni.2020.10.011.

52. J. Ochando, W. J. M. Mulder, J. C. Madsen, M. G. Netea, and R. Duivenvoorden, "Trained Immunity — Basic Concepts and Contributions to Immunopathology," *Nature Reviews Nephrology* 19, no. 1 (2023): 23–37, https://doi.org/10.1038/s41581-022-00633-5.

53. Y. Chen, R. Liang, Y. Li, et al., "Chromatin Accessibility: Biological Functions, Molecular Mechanisms and Therapeutic Application," *Stem Cell Research & Therapy* 9, no. 1 (2024): 1–39, https://doi.org/10.1038/s41392-024-02030-9.

54. S. Y. Thomas, G. S. Whitehead, M. Takaku, et al., "MyD88-Dependent Dendritic and Epithelial Cell Crosstalk Orchestrates Immune Responses to Allergens," *Mucosal Immunology* 11, no. 3 (2018): 796–810, https://doi.org/10.1038/mi.2017.84.

55. M. J. Schuijs, M. A. Willart, K. Vergote, et al., "Farm Dust and Endotoxin Protect Against Allergy Through A20 Induction in Lung Epithelial Cells," *Science* 349, no. 6252 (2015): 1106–1110, https://doi.org/10.1126/science.aac6623.

56. R. D. Weeratna, C. L. Brazolot Millan, M. J. McCluskie, and H. L. Davis, "CpG ODN Can Re-Direct the Th Bias of Established Th2 Immune Responses in Adult and Young Mice," *FEMS Immunology & Medical Microbiology* 32, no. 1 (2001): 65–71, https://doi.org/10.1111/j.1574-695X.2001.tb00535.x.

57. V. Pivniouk, J. A. Gimenes-Junior, P. Ezeh, et al., "Airway Administration of OM-85, a Bacterial Lysate, Blocks Experimental Asthma by Targeting Dendritic Cells and the Epithelium/IL-33/ILC2 Axis," *Journal of Allergy and Clinical Immunology* 149, no. 3 (2022): 943–956, https://doi.org/10.1016/j.jaci.2021.09.013.

58. M. Pereira and R. T. Gazzinelli, "Regulation of Innate Immune Signaling by IRAK Proteins," *Frontiers in Immunology* 14 (2023): 1133354, https://doi.org/10.3389/fimmu.2023.1133354.

59. M. J. Hossen, W. S. Yang, D. Kim, A. Aravinthan, J. H. Kim, and J. Y. Cho, "Thymoquinone: An IRAK1 Inhibitor With In Vivo and In Vitro Anti-Inflammatory Activities," *Scientific Reports* 7 (2017): 42995, https://doi.org/10.1038/srep42995.

60. E. S. M. Ammar, N. M. Gameil, N. M. Shawky, and M. A. Nader, "Comparative Evaluation of Anti-Inflammatory Properties of Thymoquinone and Curcumin Using an Asthmatic Murine Model," *International Immunopharmacology* 11, no. 12 (2011): 2232–2236, https://doi.org/10.1016/j.intimp.2011.10.013.

61. H. Ahmed, M. A. Khan, U. D. Kahlert, et al., "Role of Adaptor Protein Myeloid Differentiation 88 (MyD88) in Post-Subarachnoid Hemorrhage Inflammation: A Systematic Review," *International Journal of Molecular Sciences* 22, no. 8 (2021): 4185, https://doi.org/10.3390/ijms2208-4185.

62. X. Liu, J. G. Chen, M. Munshi, et al., "Mutated MYD88 Regulates HCK Pro-Survival Signaling Through JunB in MYD88 Mutated B-Lymphoma Cells," *Blood* 134, no. S1 (2019): 3778, https://doi.org/10.1182/blood-2019-130885.

63. B. Hartenstein, S. Teurich, J. Hess, J. Schenkel, M. Schorpp-Kistner, and P. Angel, "Th2 Cell-Specific Cytokine Expression and Allergen-Induced Airway Inflammation Depend on JunB," *Embo Journal* 21, no. 23 (2002): 6321–6329, https://doi.org/10.1093/emboj/cdf648.

64. M. G. Daskalaki, C. Tsatsanis, and S. C. Kampranis, "Histone Methylation and Acetylation in Macrophages as a Mechanism for Regulation of Inflammatory Responses," *Journal of Cellular Physiology* 233, no. 9 (2018): 6495–6507, https://doi.org/10.1002/jcp.26497.

65. M. Merarchi, G. Sethi, M. K. Shanmugam, L. Fan, F. Arfuso, and K. S. Ahn, "Role of Natural Products in Modulating Histone Deacetylases in Cancer," *Molecules* 24, no. 6 (2019): 1047, https://doi.org/10.3390/molecules24061047.

66. W. B. Zhang, F. Yang, Y. Wang, et al., "Inhibition of HDAC6 Attenuates LPS-Induced Inflammation in Macrophages by Regulating Oxidative Stress and Suppressing the TLR4-MAPK/NF-κB Pathways," *Biomedicine & Pharmacotherapy* 117 (2019): 109166, https://doi.org/10.1016/j.biopha.2019.109166.

67. W. Chong, Y. Li, B. Liu, et al., "Histone Deacetylase Inhibitor SAHA Attenuates TLR4 Signaling in LPS-Stimulated Mouse Macrophages," *Journal of Surgical Research* 178, no. 2 (2012): 851–859, https://doi.org/10.1016/j.jss.2012.07.023.

68. T. Kawai, O. Adachi, T. Ogawa, K. Takeda, and S. Akira, "Unresponsiveness of MyD88-Deficient Mice to Endotoxin," *Immunity* 11, no. 1 (1999): 115–122, https://doi.org/10.1016/S1074-7613(00)80086-2.

69. O. Adachi, T. Kawai, K. Takeda, et al., "Targeted Disruption of the *MyD88* Gene Results in Loss of IL-1- and IL-18-Mediated Function," *Immunity* 9, no. 1 (1998): 143–150, https://doi.org/10.1016/S1074-7613(00)80596-8.

70. H. Menden, S. Xia, S. M. Mabry, et al., "Histone Deacetylase 6 Regulates Endothelial MyD88-Dependent Canonical TLR Signaling, Lung Inflammation, and Alveolar Remodeling in the Developing Lung," *American Journal of Physiology-Lung Cellular and Molecular Physiology* 317, no. 3 (2019): L332–L346, https://doi.org/10.1152/ajplung.00247.2018.

71. V. Y. Alfaro, D. L. Goldblatt, G. R. Valverde, et al., "Safety, Tolerability, and Biomarkers of the Treatment of Mice With Aerosolized Toll-Like Receptor Ligands," *Frontiers in Pharmacology* 5 (2014): 8, https://doi.org/10.3389/fphar.2014.00008.

72. S. E. Evans, M. J. Tuvim, C. J. Fox, N. Sachdev, L. Gibiansky, and B. F. Dickey, "Inhaled Innate Immune Ligands to Prevent Pneumonia," *British Journal of Pharmacology* 163, no. 1 (2011): 195–206, https://doi.org/10.1111/j.1476-5381.2011.01237.x.

73. M. Martin, "Cutadapt Removes Adapter Sequences From High-Throughput Sequencing Reads," *EMBnet.journal* 17, no. 1 (2011): 10–12, https://doi.org/10.14806/ej.17.1.200.

74. D. Kim, B. Langmead, and S. L. Salzberg, "HISAT: A Fast Spliced Aligner With Low Memory Requirements," *Nature Methods* 12, no. 4 (2015): 357–360, https://doi.org/10.1038/nmeth.3317.

75. M. Pertea, G. M. Pertea, C. M. Antonescu, T. C. Chang, J. T. Mendell, and S. L. Salzberg, "StringTie Enables Improved Reconstruction of a Transcriptome From RNA-seq Reads," *Nature Biotechnology* 33, no. 3 (2015): 290–295, https://doi.org/10.1038/nbt.3122.

76. M. I. Love, W. Huber, and S. Anders, "Moderated Estimation of Fold Change and Dispersion for RNA-seq Data With DESeq2," *Genome Biology* 15, no. 12 (2014): 550, https://doi.org/10.1186/s13059-014-0550-8.

77. M. D. Robinson, D. J. McCarthy, and G. K. Smyth, "edgeR: A Bioconductor Package for Differential Expression Analysis of Digital Gene Expression Data," *Bioinformatics* 26, no. 1 (2010): 139–140, https://doi.org/10.1093/bioinformatics/btp616.

78. D. R. Little, A. M. Lynch, Y. Yan, H. Akiyama, S. Kimura, and J. Chen, "Differential Chromatin Binding of the Lung Lineage Transcription Factor NKX2-1 Resolves Opposing Murine Alveolar Cell Fates In Vivo," *Nature Communications* 12, no. 1 (2021): 2509, https://doi.org/10.1038/s41467-021-22817-6.

79. T. Stuart, A. Butler, P. Hoffman, et al., "Comprehensive Integration of Single-Cell Data," *Cell* 177, no. 7 (2019): 1888–1902.e21, https://doi.org/10.1016/j.cell.2019.05.031.

80. D. R. Little, K. N. Gerner-Mauro, P. Flodby, et al., "Transcriptional Control of Lung Alveolar Type 1 Cell Development and Maintenance by NK Homeobox 2-1," *Proceedings of the National Academy of Science of United States of America* 116, no. 41 (2019): 20545–20555, https://doi.org/10.1073/pnas.1906663116.

81. G. Finak, A. McDavid, M. Yajima, et al., "MAST: A Flexible Statistical Framework for Assessing Transcriptional Changes and Characterizing Heterogeneity in Single-Cell RNA Sequencing Data," *Genome Biology* 16 (2015): 278, https://doi.org/10.1186/s13059-015-0844-5.

Supporting Information

Additional supporting information can be found online in the Supporting Information section.

Supporting File: eji70172-sup-0001-SupMat.pdf.